Specific Binding Sites for Cations in Bacteriorhodopsin

Tamar Eliash,* Lev Weiner,† Michael Ottolenghi,‡ and Mordechai Sheves*
Departments of *Organic Chemistry and †Chemical Services, Weizmann Institute of Science, Rehovot 76100, Israel; and ‡Department of Physical Chemistry, The Hebrew University of Jerusalem, Jerusalem 91904, Israel

ABSTRACT The Asp-85 residue, located in the vicinity of the retinal chromophore, plays a key role in the function of bacteriorhodopsin (bR) as a light-driven proton pump. In the unphotolyzed pigment the protonation of Asp-85 is responsible for the transition from the purple form (λ_{max} = 570 nm) to the blue form (λ_{max} = 605 nm) of bR. This transition can also be induced by deionization (cation removal). It was previously proposed that the cations bind to the bR surface and raise the surface pH, or bind to a specific site in the protein, probably in the retinal vicinity. We have reexamined these possibilities by evaluating the interaction between Mn^{2+} and a nitroxyl radical probe covalently bound to several mutants in which protein residues were substituted by cystein. We have found that Mn^{2+}, which binds to the highest-affinity binding site, significantly affects the EPR spectrum of a spin label attached to residue 74C. Therefore, it is concluded that the highest-affinity binding site is located in the extracellular side of the protein and its distance from the spin label at 74C is estimated to be ~9.8 ± 0.7 Å. At least part of the three to four low-affinity cation binding sites are located in the cytoplasmic side, because Mn^{2+} bound to these binding sites affects spin labels attached to residues 103C and 163C located in the cytoplasmic side of the protein. The results indicate specific binding sites for the color-controlling cations, and suggest that the binding sites involve negatively charged lipids located on the exterior of the bR trimer structure.

INTRODUCTION

Bacteriorhodopsin (bR) is the light-transducing protein in the purple membrane of *Halobacterium salinarum* (Oesterhelt and Stoeckenius, 1971, 1974). The protein contains an all-*trans* retinal chromophore bound covalently via a protonated Schiff base to Lys-216. Following light absorption, bR converts from a dark-adapted state containing a mixture of 13-*cis* and all-*trans* retinal to a light-adapted state that contains only the all-*trans* chromophore. Light absorption by the light-adapted state initiates a photocycle characterized by several distinct intermediates. The photocycle is coupled to proton release to the extracellular medium, a step that initiates a proton pump cycle. The formed pH gradient generates a proton-motive force that is used by the bacterium to synthesize ATP from inorganic phosphate and ADP. The proton pumping process is initiated by a proton transfer from the retinal-protonated Schiff base linkage, which generates the blue-shifted M photocycle intermediate (for recent reviews see Ottolenghi and Sheves, 1995; Lanyi, 1997; Haupts et al., 1999).

Lowering the pH of bacteriorhodopsin suspension red-shifts the pigment absorption maximum from 565 nm to 605 nm and produces a blue membrane (Mowery et al., 1979; Fischer and Oesterhelt, 1979; Edgerton et al., 1980; Kimura et al., 1984; Váró and Lanyi, 1989). This transition from purple to blue membrane is characterized by pK_a = 2.7 in 0.1 M NaCl (Kimura et al., 1984; Chang et al., 1985) and is referred to as blue membrane state produced at low pH (Kobayashi et al., 1983; Dupuis et al., 1985; Albeck et al., 1989; Nasuda-Kouyama et al., 1990). It was found that the formation of the blue membrane is associated with protonation of Asp-85, which probably induces the spectrum red shift, due to elimination of the electrostatic interaction between the retinal protonated Schiff base and Asp-85 (Metz et al., 1992).

Removal of cations by deionization treatment produces "deionized blue membrane" (Padros et al., 1984; Chang et al., 1985; Jonas and Ebrey, 1991) characterized by higher purple to blue pK_a, which is similar to the acid blue form. Therefore, cations play an important role in bR function, and it was suggested that they control the pK_a of Asp-85 residue, thereby allowing for production of the crucial M intermediate in the photocycle (Kobayashi et al., 1983; Moltke and Heyn, 1995). Furthermore, it was suggested that cations participate in the mechanism that controls the proton transfer following light absorption (Tan et al., 1996; Birge et al., 1996). A variety of experimental data suggested specific cation binding to bR. Potentiometric titration studies of deionized membrane using a Ca^{2+}-specific electrode have suggested two high-affinity cation binding sites and four to six low-affinity sites (Zhang et al., 1992, 1993; Zhang and El-Sayed, 1993; Yang and El-Sayed, 1995; Yoo et al., 1995). It was proposed that the binding of cations of the second high-affinity site correlates with the blue-purple transition (Ariki and Lanyi, 1986; Zhang et al., 1992). EPR measurement of Mn^{2+} indicated one high-affinity and three weaker binding sites, characterized by similar binding constants (Dunach et al., 1987).

Several studies have suggested that the cation binding site, which determines the state of protonation of Asp-85

Received for publication 6 February 2001 and in final form 16 April 2001.
Address reprint requests to Dr. Mordechai Sheves, Dept. of Organic Chemistry, Weizmann Institute of Science, Rehovot 76100, Israel. Tel.: 972-8-9344320; Fax: 972-8-9344142; E-mail: mudi.sheves@weizmann.ac.il, or to Dr. Michael Ottolenghi, Dept. of Physical Chemistry, The Hebrew University of Jerusalem, Jerusalem 91904, Israel. Tel.: 972-2-6585335; Fax: 972-2-6524951; E-mail: micott@chem.ch.huji.ac.il.

0006-3495/01/08/1155/08 $2.00

and, thus, the color of the pigment, is located in the retinal binding pocket (Jonas and Ebrey, 1991; Zhang et al., 1992; Tan et al., 1996; Pardo et al., 1998). Another model suggested that the cations bind to the membrane surface and control the apparent pK_a of Asp-85, thereby the purple-blue transition through surface potential effects (Szundi and Stoeckenius, 1987–1989). Free (Guy-Chapman) or bound metal cations on the membrane surface compete with protons and thus determine the local proton concentration around the membrane.

Recently, kinetic studies of Asp-85 reprotonation as a function of cation size have indicated that the color-controlling cation binding site is in an exposed location on or close to the membrane surface (Fu et al., 1997). Furthermore, it was shown that the titrations of Asp-85 and of the cation binding residues in bR are uncoupled, excluding direct binding of the cation to Asp-85 (Eliash et al., 1999). Solid-state NMR studies indicated that cation binding affects Ala-196 located in the E-F interhelical loop, supporting binding in the membrane surface (Tuzi et al., 1999). A study using eosin dye covalently bound to the protein suggested that the cations do not bind to specific sites and bind equally to both membrane surfaces to negatively charged lipids (Váró et al., 1999).

In this study we have reexamined the possibility of specific cation binding sites using a new, complementary approach. We have monitored the interaction between Mn^{2+} and EPR probe, covalently bound to several mutants in which protein residues were substituted by cystein, and have revealed that the high-affinity binding site is located in the extracellular region, whereas at least part of the three to four low-affinity cation binding sites are located in the cytoplasmic surface. The results indicate specific binding sites for the color-controlling cations and suggest that all the cation binding sites are associated with negatively charged lipids located on the exterior of the bR trimer structure.

MATERIALS AND METHODS

Bacteriorhodopsin mutants were obtained as a generous gift from Prof. R. Needleman of Wayne State University.

Spin-labeled mutants

The radical probe was attached to three different mutants by forming a covalent bond between a specific cysteine mutation and the radical. The spin label (1-oxyl-2,2,5,5-tetramethylpyrroline-3-methyl)-methanethiosulfonate (MTSSL, Toronto Research Chemicals, Ontario, Canada), was covalently attached to cysteine residue of the appropriate bR mutant (A103C, M163C, or E74C) to yield the spin label side chain. A 10-fold excess of the radical was used in 0.1 M phosphate buffer (pH 8) and 0.1 M NaCl. The suspensions were stirred at room temperature for 12 h. The non-covalently bound spin label was removed by washing the membrane pellet with a solution of 1% BSA.

Spin-labeled artificial pigment *I*

The nitroxide retinal analog was synthesized from 2,2,5,5-tetramethyl-3-pyrroline-1-oxyl-3-carboxylic acid according to previously described procedures (Crouch et al., 1981). The synthetic retinal analog was incubated with apomembrane for 3–6 h at room temperature to yield pigment **I**, which absorbs at 460 nm (Crouch et al., 1981).

Deionized (DI) blue membranes were obtained by passing bR suspension or the appropriate labeled mutants and the artificial pigment **I** through a Dowex 50 WX8 (Fluka, Buchs, Switzerland) cation exchange column.

EPR measurements and distance calculations

Increasing Mn^{2+} concentrations were added to deionized membrane samples, and the EPR spectra of both the radical probe and the Mn^{2+} free signal were monitored. The pH was adjusted to 5 and readjusted using NaOH solution with each addition of Mn^{2+}.

The EPR measurements were preformed on a Bruker ER200 D-SRC. The samples were measured at a concentration of $\sim 5 \times 10^{-5}$ M radial probe.

Distance calculations

The distance between nitroxyl spin label and bound Mn^{2+} was estimated by measuring the intensity decrease of the EPR signal of the spin-labeled protein (central component) upon addition of Mn^{2+} (Leigh, 1970; Voss et al., 1995). The distance, R, was calculated from the following equation (Leigh, 1970):

$$R = \sqrt[6]{\frac{g\beta\mu^2}{\hbar c} \cdot \tau_c} \qquad (1)$$

The constant g is the electronic factor for nitroxyl radical, β is the Bohr magneton, and μ and τ_c are the magnetic moment and the electron-spin relaxation time of Mn^{2+}. $\tau_c = 1.5 \times 10^{-9}$ s (Cohn et al., 1971) was used. The value of c/H_o was obtained from the relative amplitude (I/I_o) of EPR spectrum of the spin label in the presence of paramagnetic ion using a graph presented by Voss et al. (1995) for the label motion in solution (isotropic case). In this graph we used H_o (line width of central component of the EPR spectrum) as $H_o = 2$ G for mutant E74C, and $H_o = 6$ G for M163C and A103C.

RESULTS

Binding of Mn^{2+} to deionized wild-type and mutants E74C, A103C, and M163C

The binding of Mn^{2+} to deionized protein membranes was followed by an EPR spectrum. The spectrum mostly originates from unbound Mn^{2+} because the amplitude of the bound Mn^{2+} is only $\sim$5% of that of an identical concentration of the free ion in solution. Three mutants, E74C, A103C, and M163C, were spin-labeled by (1-oxyl-2,2,5,5-tetramethylpyrroline-3-methyl)-methanethiosulfonate (Aharoni et al., 2000) and their EPR spectra are shown in Fig. 1.

The relatively sharp peaks of the labeled E74C mutant compared with the other mutants indicate that the probe movement in this position is less restricted by the protein's environment, and increased free rotation is achieved.

Scatchard plots of Mn^{2+} binding to blue membranes (Fig. 2) indicate that all three mutants are characterized by one

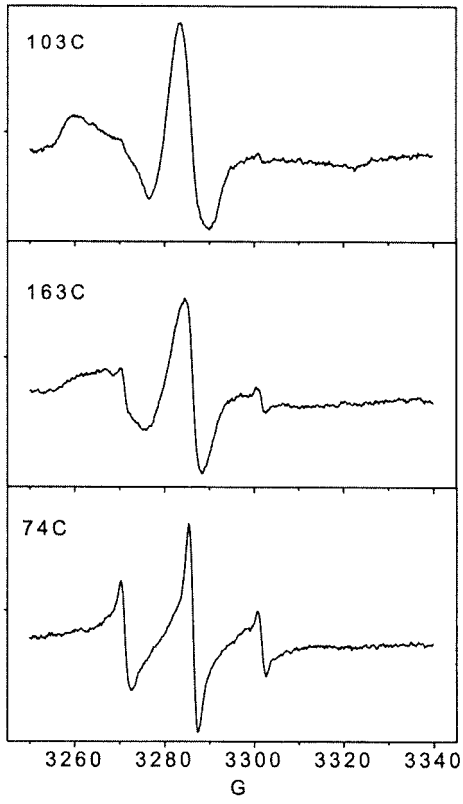

FIGURE 1 EPR spectra of spin-labeled bR mutants A103C, M163C, and E74C. Protein concentration: 8×10^{-5} M, $T = 23$°C.

strong binding site (Table 1) and by three or four additional, identically weaker binding sites similarly to the wild type (Dunach et al., 1987). Interestingly, the first strong binding site did not follow a simple binding behavior (Fig. 2 *A* for the three mutants, and Fig. 2 *B* for wild type), and it appears that the first cation binds in a cooperative manner. A Scatchard plot of ν/c versus ν (ν, number of Mn^{2+} equivalents bound to bR; c, concentration of added Mn^{2+}) should give a straight line with a slope of $-K$ (binding constant), while the x intercept yields the value of n (number of binding sites with the same affinity), according to:

$$\nu/c = K(n - \nu) \quad (2)$$

To exclude the possibility that the effect on the EPR spectrum does not originate from a protein conformational change, due to blue-purple transition, we carried out a control experiment. Binding of Ca^{2+} instead of Mn^{2+} to the blue membrane did not affect the EPR spectrum. This experiment clearly indicates the role of magnetic interaction between the paramagnetic species in decreasing the EPR spectrum intensity.

It is clear (Fig. 2, *A* and *B*) that the first Mn^{2+} equivalent deviates from the expected behavior and the binding is stronger as more Mn^{2+} is added. Further studies should be carried out to clarify this observation and its origin. Mutants 74C and 163C exhibited, in addition to the strong binding site, three weaker sites in contrast to mutant 103C, which exhibited four weaker sites.

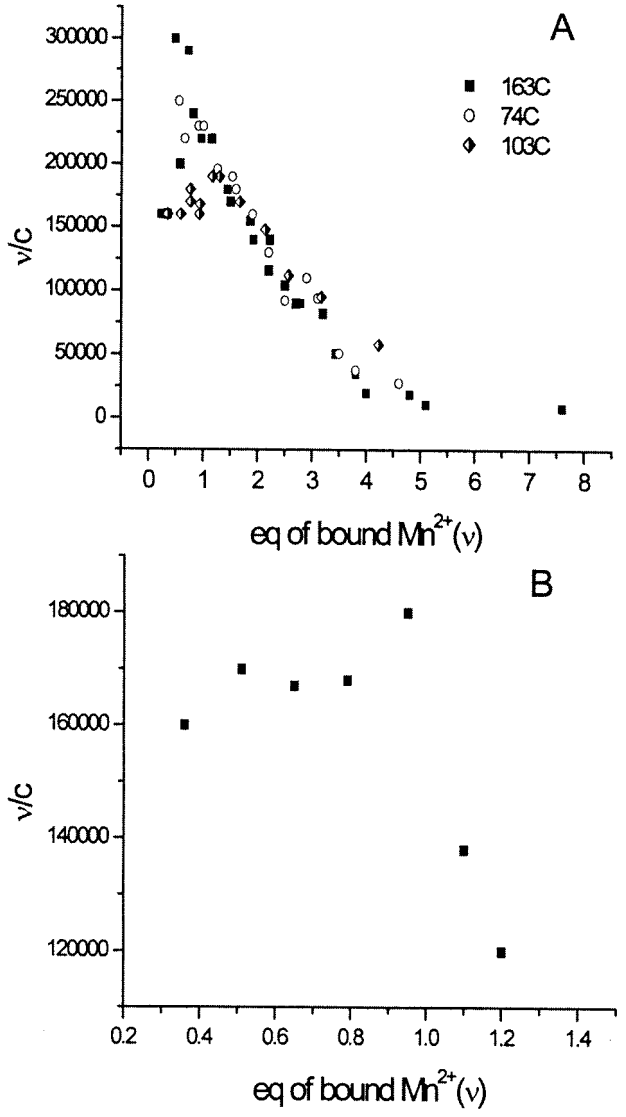

FIGURE 2 Scatchard plots of Mn^{2+} binding to deionized bR mutants and native bR at pH 5. The concentration of free Mn^{2+} in the solution was determined by the EPR spectra. The bound EPR signal of Mn^{2+} was only ~5% of the free EPR Mn^{2+} signal. (*A*) Mutants M163C, E374C, and A103C. (*B*) Scatchard plot of the high-affinity binding site of native bR.

Effect of Mn^{2+} binding on the EPR probe signal

Binding Mn^{2+} to the blue membrane forms of the mutants reduces the signal of the EPR probe due to dipole-dipole

TABLE 1 Binding constants of the two classes of binding sites in the various mutants

Mutant	K_1 (M^{-1})	n_1	K_2 (M^{-1})	n_2
163C	2.2×10^5	1	6.8×10^4	3
103C	1.7×10^5	1	4.5×10^4	4
74C	2.2×10^5	1	6.6×10^4	3

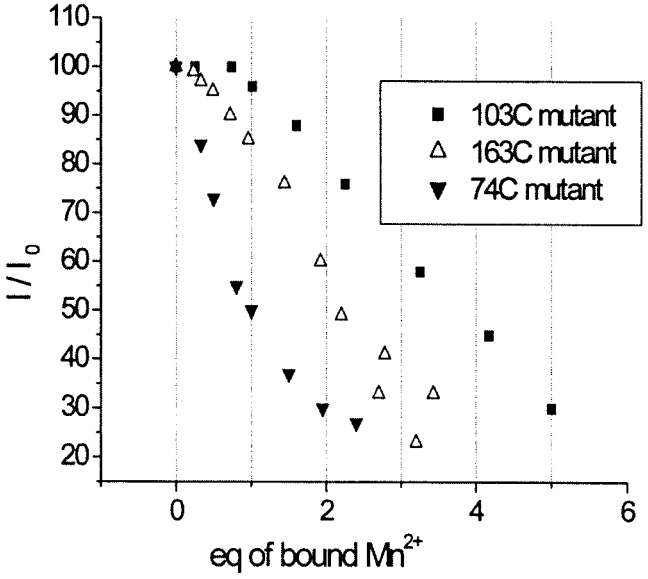

FIGURE 3 Effect of Mn^{2+} binding to deionized bR mutants on the central component of the EPR spectra of labeled mutants A103C, E74C, and M163C.

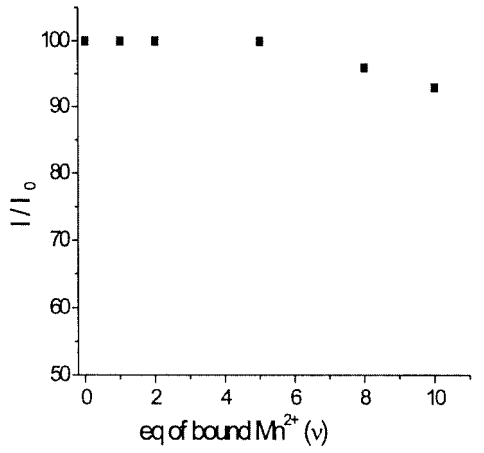

FIGURE 4 Effect of Mn^{2+} binding to deionized artificial bR I on the central component of the EPR spectrum.

interactions between the bound Mn^{2+} and the probe. The interaction strength is correlated with the distance between the paramagnetic species (see Eq. 1). In the labeled 74C mutant located in the extracellular side, the first equivalent of Mn^{2+} significantly affects the EPR signal (Fig. 3) and lowers its intensity by ~50%. The second equivalent of Mn^{2+} further reduces the signal to ~30% of the original signal (Fig. 3). Different behavior was observed for the 103C mutant located at the cytoplasmic side (Pebay-Peyroula et al., 1997; Luecke et al., 1998). The first equivalent of Mn^{2+} had a minor effect and reduced the signal intensity by only ~8%, whereas an additional four equivalents affected the signal more significantly and reduced it monotonically up to 30% of the original signal (Fig. 3).

In mutant 163C, which is located on the cytoplasmic side, the first equivalent of Mn^{2+} reduced the EPR probe signal by ~15% and further addition of two equivalents reduced the main EPR signal more significantly, up to 20% of its original intensity. These experiments clearly indicate that the three labeled mutants are affected differently by the bound Mn^{2+} cations.

To gain further information on binding site locations of the Mn^{2+} cations we prepared artificial pigment **I**, derived from a retinal analog characterized by a spin-labeled substitution of the native retinal β-ionone ring (Crouch et al., 1981). Binding of five Mn^{2+} equivalents to deionized pigment **I** (as evident from the EPR spectra of Mn^{2+}) did not affect the intensity of the EPR signal. A minor effect of ~10% peak reduction was obtained by an additional binding of five equivalents (Fig. 4). We note that the EPR data indicated similar Mn^{2+} binding to both pigment **I** and native bR. This very weak effect on the EPR signal clearly indicates that the cations do not bind to the retinal chromophore vicinity and supports earlier suggestions (Szundi and Stoeckenius, 1987) and our recent results that the cations bind on or close to the membrane surface (Fu et al., 1997; Eliash et al., 1999).

Estimation of the distance of the Mn^{2+} cation from the EPR probe

Leigh methodology (Leigh, 1970) allows for distance estimation between a paramagnetic cation and the nitroxyl radical probe. Analysis in the bacteriorhodopsin system is more complicated and requires several assumptions because it involves the binding of more than one cation. The strongest binding site mostly affects the 74 residue and, assuming that two equivalents of Mn^{2+} lead to almost complete occupation of the high-affinity binding site, the calculated distance of the Mn^{2+} cation for the EPR probe is ~9.8 ± 0.7 Å. The situation is more complicated for the three to four low-affinity binding sites because interaction of Mn^{2+} with the spin label will be the sum of the contributions of each Mn^{2+} that produces a paramagnetic effect (Hill et al., 1988), and many combinations are possible for the distances between the Mn^{2+} and 103 and 106 residues. To estimate the topographical relationship we used the extreme case in which all the low-affinity binding sites were equidistant from the spin label and, therefore, all affect the spin-probe

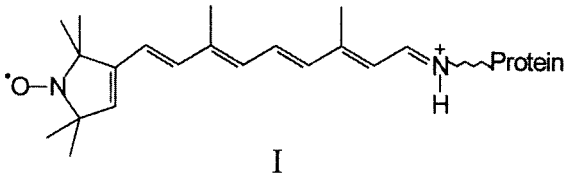

I

Scheme 1.

EPR spectrum. Assuming full occupation by three and four equivalents for 103C and 163C mutants, we obtained an average distance of ~15.1 ± 0.7 Å and 13.2 ± 0.7 Å of the binding sites from 103 and 163 residues, correspondingly.

DISCUSSION

Several studies have led to the suggestion that the high-affinity binding site for cations, which is responsible for the blue-purple transition, is located in the vicinity of the retinal protonated Schiff base associated with Asp-85 and Asp-212 residues (El-Sayed et al., 1995; Jonas and Ebrey, 1991; Stuart et al., 1995; Tan et al., 1996). In contrast, another approach proposed that the cations bind to the membrane surface and their effect on the purple → blue equilibrium was attributed to surface potential effects (Szundi and Stoeckenius, 1987). We have recently examined the kinetics of Asp-85 reprotonation as a function of cation size. The studies suggest that the color-controlling cation binding site is in an exposed location on or close to the membrane surface (Fu et al., 1997). These studies are supported by the observation that the titration of Asp-85 and the binding residues of the cation are not coupled (Eliash et al., 1999).

Recent studies with eosin dye covalently linked to the protein and ^{13}C-NMR studies (Váró et al., 1999; Tuzi et al., 1999) supported the suggestion that a cation does not bind specifically to the retinal binding site. Furthermore, none of the high-resolution diffraction studies identified a divalent cation at the chromophore binding site (Kimura et al., 1997a, b; Pebay-Peyroula et al., 1997; Luecke et al., 1998; Essen et al., 1998). However, because these studies did not identify any cation in the structure, it seems plausible that the method of sample preparation eliminated the cations that usually bind to bacteriorhodopsin. The results described in the present work strongly indicate that the cation binding sites are not located within the retinal vicinity. The insensitivity of the radical probe, EPR signal of pigment **I** tailored into the retinal binding site to interaction with the Mn^{2+} dipole occupying the five high-affinity binding sites, indicates that the distance between the two paramagnetic species is >22 Å. This is in keeping with cation binding sites on or close to the membrane surface.

Before discussing in more detail the identity and locations of the cation binding site, we point out that the following analysis is based on three plausible assumptions: 1) Mn^{2+} occupies the same binding site as Ca^{2+} or Mg^{2+} do in native bR, though with a somewhat different binding constant (Dunach et al., 1987). 2) The present mutations do not markedly affect the bR structure to modify the cation binding sites and their respective affinities. This assumption is supported by the similarity of the respective Scatchard plots (Dunach et al., 1987 and the present work). 3) Although regenerated Ca^{2+}-bR is found to exhibit some changes in protein structure with respect to native bR (Tuzi et al., 1999), we assume that the identities of the cation binding sites are the same in both systems.

We refer to the observation (see Fig. 2) of a change in the sign of the slopes of the Scatchard plots around $\nu = 1$. Such a deviation from a simple expected behavior may be indicative of a cooperative binding mechanism in which the binding constant of the site in one trimer member is affected (increases) upon populating the site of a neighboring member of the trimer. An alternative explanation may be advanced on the basis of the model (Szundi and Stoeckenius, 1987–1989) based on the effects of cations on the surface pH of the bR membrane. When the first few cations are bound the surface pH increases. This reduces competition by protons, increasing the apparent cation affinity to the (same) binding site. Finally, one cannot exclude the possibility of two interacting biding sites that are populated in parallel up to a 50% population. Nevertheless, the discussion below is based on the more likely assumption that at $\nu = 1$ mostly one high-affinity site is populated.

Quenching of the radical probe EPR signal by the first equivalent of Mn^{2+}, which is added to the deionized membrane, is much more efficient in the 74C-labeled pigment than in the 103C and 163C, indicating that the highest-affinity binding site is located on the extracellular side of the protein. The binding constants ratio of the strongest binding site and the weaker three, in the 74C-labeled pigment, is ~3:1 (Table 1). Therefore, only ~75% of the highest-affinity binding site will be occupied by the first Mn^{2+} equivalent and almost complete occupation will occur following addition of the second equivalent. The observation that ~70% of the EPR signal is quenched by two equivalents of Mn^{2+} indicates that the distance between Mn^{2+} and the probe labeled at the 74C residue is 9.8 ± 0.7 Å. The binding constant ratio of the highest- and low-affinity binding sites for mutants 103C and 163C is ~3:1 (Table 1). Therefore, only ~25% of the first equivalent of Mn^{2+} will be distributed among the weaker binding sites, whereas additional equivalents will populate mostly the weaker binding site. Indeed, the first equivalent of Mn^{2+} effects the EPR label at 103C and 163C more weakly than an additional two or three equivalents. The EPR signal is quenched by only 8% (103C) and 15% (163C) by the first equivalent, whereas two equivalents quenched the signal by 25% and 50%. The results contradict nonspecific binding to both extracellular and cytoplasmic sides, and are in keeping with specific cation binding sites in which the highest-affinity binding site is located on the extracellular site where 74C residue is located. The low affinity of the sites on the cytoplasmic side can be interpreted in terms of an intrinsically weak binding sites. Alternatively, adopting the approach of Szundi and Stoeckenius (1987–1989), it could be attributed to a lower surface pH on that side of the membrane. However, the different sensitivity of the EPR probe at residues 103C and 163C to Mn^{2+} interaction indicate specific locations for the cation binding sites that could

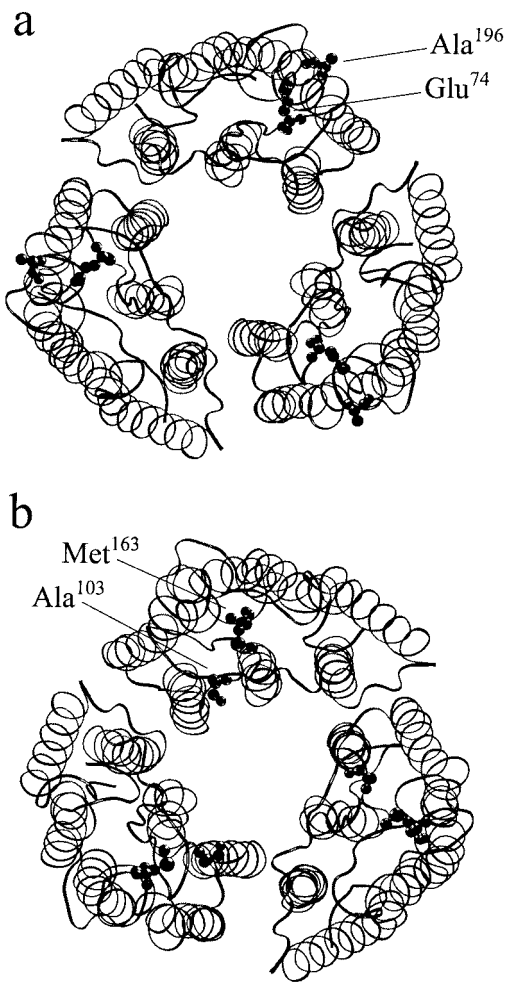

FIGURE 5 Bacteriorhodopsin trimer structure. The coordinates of Essen et al. (1998) were used (1BRR). (*a*) Cytoplasmic view, Glu-74 and Ala-196 are labeled for one monomer. (*b*) Extracellular view, Met-163 andAla-103 are labeled for one bR monomer.

result from an asymmetric distribution of lipids (Essen et al., 1998).

Recent ^{13}C-NMR studies suggested that one of the preferred cation-binding sites is located at the loop between helices F and G near Ala-196 (Tuzi et al., 1999). These results are consistent with our present observation. Residue 74C is located in the inner part of the trimer structure of bR (Kimura et al., 1997a, b; Pebay-Peyroula et al., 1997; Luecke et al., 1998; Essen et al., 1998). The strong influence of Mn^{2+} on residue Ala-196 labeled with ^{13}C and the distance of 9.8 $\pm$ 0.7 Å we have found between Mn^{2+}-labeled residues, point to the highest-affinity binding site being located in the protein extracellular side at the exterior of the trimer structure (Fig. 5 *a*). Both labels at 163C and 103C are affected far less by the first equivalent of Mn^{2+}, in keeping with the suggestion that the highest-affinity binding site is located at the extracellular side. The low-affinity three to four additional binding sites are located at the protein cytoplasmic side, as is evident by the Mn^{2+} influence on the EPR signal of labels at 163C and 103C. We note that we cannot exclude the possibility that one or two of the low-affinity binding sites are located at the extracellular side. In this case, the effect on 163 and 103 labeled residues originated from part of the low-affinity binding sites, whereas the effect on the spin label at the 74 residue, located in the extracellular side, was negligible because the signal was almost completely quenched by the Mn^{2+} occupying the high-affinity binding site. 163C is located closer to the exterior of the trimer structure than 103C (Fig. 5 *b*). The average distance calculated between the low-affinity binding sites and these residues (13.2 $\pm$ 0.7 and 15.2 $\pm$ 0.7 Å) do not contradict the fact that these binding sites are located in the exterior of the trimer structure. Therefore, it is tempting to speculate that both the strongest cation binding site and the three to four weaker sites are located on the exterior of the trimer, and probably involve the membrane acidic groups and, possibly, protein residues. This suggestion is in keeping with a previous observation that bR treated with CHAPS lacks the cation binding sites discussed above (Eliash et al., 1999). Previous studies indicated that deoxycholate-treated purple membrane, in which a partially delipidated process occurred, maintained the original native purple membrane trimer structure (Grigorieff et al., 1995). Three of the lipids per bR molecule remain in an identical position relative to the trimer and, in addition, three lipids per bR molecule have been identified, including a lipid between the monomers. Part of the lipids on the trimer exterior was removed by deoxycholate treatment. Partial lipid-depleted membranes obtained by CHAPS treatment exhibit a normal circular dichroism spectrum (data not shown), indicating that the trimer structure is intact, as was observed for the deoxycholate-treated purple membrane. Therefore, since the CHAPS-treated purple membrane lost its ability to bind cations (Eliash et al., 1999), it is tempting to suggest that the strong cation binding sites are located on the exterior of the trimers and are associated with negatively charged lipids, but not with the lipids occluded inside the trimers or between the monomers.

Our results, revealing specific binding sites for the strong cation binding sites, seem to contradict recent experiments that used eosin dye (Váró et al., 1999). These experiments indicated that the surface pH changes about equally at both extracellular and cytoplasmic surfaces when one equivalent of Ca^{2+} is added to the blue membrane. However, the eosin dye bound to the cytoplasmic side may respond to binding at the extracellular side, because it was reported that released protons on the extracellular side of bR rapidly equilibrate with the cytoplasmic side (Heberle et al., 1994; Alexiev et al., 1995). It is possible that this equilibration process prevents different proton concentrations at both sides of the membrane.

The work was supported by the A.M.N. Fund for the Promotion of Science, Culture and Arts in Israel; the U.S.-Israel Binational Science Foundation; the Israel National Science Foundation administered by the Israel Academy of Sciences and Humanities; and the Human Frontier Science Program.

REFERENCES

Aharoni, A., L. Weiner, M. Ottolenghi, and M. Sheves. 2000. Bacteriorhodopsin experiences light-induced conformational alterations in non-isomerizable $C_{13}{=}C_{14}$ pigments. *J. Biol. Chem.* 275:21010–21016.

Albeck, A., N. Friedman, M. Sheves, and M. Ottolenghi. 1989. Factors affecting the absorption maxima of acidic forms of bacteriorhodopsin. A study with artificial pigments. *Biophys. J.* 56:1259–1265.

Alexiev, U., R. Mollaaghababa, P. Scherrer, H. G. Khorana, and M. P. Heyn. 1995. Rapid long-range proton diffusion along the surface of the purple membrane and delayed proton transfer into the bulk. *Proc. Natl. Acad. Sci. U.S.A.* 92:372–376.

Ariki, M., and J. K. Lanyi. 1986. Characterization of metal ion-binding sites in bacteriorhodopsin. *J. Biol. Chem.* 261:8167–8174.

Birge, R. R., D. S. K. Govender, K. C. Izgi, and E. H. L. Tan. 1996. Role of calcium in the proton pump of bacteriorhodopsin. Microwave evidence for a cation-gated mechanism. *J. Phys. Chem.* 100:9990–10004.

Chang, C. H., J. G. Chen, R. Govindjee, and T. Ebrey. 1985. Cation binding by bacteriorhodopsin. *Proc. Natl. Acad. Sci. U.S.A.* 82: 396–400.

Cohn, M., H. Diefenbach, and J. S. Taylor. 1971. Magnetic resonance studies of the interaction of spin-labeled creatine kinase with paramagnetic manganese-substrate complexes. *J. Biol. Chem.* 246:6037–6042.

Crouch, R., T. Ebrey, and R. Govindjee. 1981. Bacteriorhodopsin analogue containing the retinal nitroxide free radical. *J. Am. Chem. Soc.* 103: 7364–7366.

Dunach, M., M. Seigneuret, J. L. Rigaud, and E. Padros. 1987. Characterization of the cation binding sites of the purple membrane. Electron spin resonance and flash photolysis studies. *Biochemistry.* 26:1179–1186.

Dupuis, P., T. C. Corcoran, and M. A. El-Sayed. 1985. Importance of bound divalent cations to the tyrosine deprotonation during the photocycle of bacteriorhodopsin. *Proc. Natl. Acad. Sci. U.S.A.* 82:3662–3664.

Edgerton, M. E., T. A. Moore, and C. Greenwood. 1980. Investigations into the effect of acid on the spectral and kinetic properties of purple membrane from *Halobacterium halobium*. *Biochem. J.* 189:413–420.

Eliash, T., M. Ottolenghi, and M. Sheves. 1999. The titrations off Asp-85 and of the cation binding residues in bacteriorhodopsin. *FEBS. Lett.* 447:307–310.

El-Sayed, M., D. Yang, S. Yoo, and N. Zhang. 1995. The effect of different metal cation binding on the proton pumping in bacteriorhodopsin. *Isr. J. Chem.* 35:465–474.

Essen, L. O., R. Siegert, W. D. Lehmann, and D. Oesterhelt. 1998. Lipid patches in membrane protein oligomers: crystal structure of the bacteriorhodopsin-lipid complex. *Proc. Natl. Acad. Sci. U.S.A.* 95: 11673–11678.

Fischer, U., and D. Oesterhelt. 1979. Chromophore equilibria in bacteriorhodopsin. *Biophys. J.* 28:211–230.

Fu, X., S. Bressler, M. Ottolenghi, T. Eliash, N. Friedman, and M. Sheves. 1997. Titration kinetics of Asp-85 in bacteriorhodopsin: exclusion of the retinal pocket as the color-controlling cation binding site. *FEBS Lett.* 416:167–170.

Grigorieff, N., E. Beckmann, and F. Zemlin. 1995. Lipid location in deoxycholate-treated purple membrane at 2.6 Å. *J. Mol. Biol.* 254: 404–415.

Haupts, H., J. Tittor, and D. Oesterhelt. 1999. Closing on bacteriorhodopsin: progress in understanding the molecule. *Annu. Rev. Biophys. Biomol. Struct.* 28:367–399.

Heberle, J., J. Riesle, G. Thiedemann, D. Oesterhelt, and N. A. Dencher. 1994. Proton migration along the membrane surface and retarded surface to bulk transfer. *Nature.* 370:379–382.

Hill, K., S. Steiner, and F. Castellino. 1988. Estimation of the distance between the divalent cation binding site of des-1–41-light chain-activated bovine plasma protein C and a nitroxide spin label attached to the active-site serine residue. *Biochem. J.* 251:229–236.

Jonas, R., and T. G. Ebrey. 1991. Binding of a single divalent cation directly correlates with the blue-to-purple transition in bacteriorhodopsin. *Proc. Natl. Acad. Sci. U.S.A.* 88:149–153.

Kimura, Y., A. Ikegami, and W. Stoeckenius. 1984. Salt- and pH-dependent changes of the purple membrane absorption spectrum. *Photochem. Photobiol.* 40:641–646.

Kimura, Y., D. G. Vassylyev, A. Miyazawa, A. Kidera, M. Matsushima, K. Mitsuoka, K. Murata, T. Hirai, and Y. Fujiyoshi. 1997a. High resolution structure of bacteriorhodopsin determined by electron crystallography. *Photochem. Photobiol.* 66:764–767.

Kimura, Y., D. G. Vassylyev, A. Miyazawa, A. Kidera, M. Matsushima, K. Mitsuoka, K. Murata, T. Hirai, and Y. Fujiyoshi. 1997b. Surface of bacteriorhodopsin revealed by high-resolution electron crystallography. *Nature.* 389:206–211.

Kobayashi, T., H. Ohtani, J.-I. Iwai, A. Ikegami, and H. Uchiki. 1983. Effect of pH on the photoreaction cycles of bacteriorhodopsin. *FEBS Lett.* 162:197–200.

Lanyi, J. K. 1997. Mechanism of ion transport across membranes. Bacteriorhodopsin as a prototype for proton pumps. *J. Biol. Chem.* 272: 31209–31212.

Leigh, J. S. 1970. ESR rigid-lattice line shape in a system of two interacting spins. *J. Chem. Phys.* 52:2608–2612.

Luecke, H., H. T. Richter, and J. K. Lanyi. 1998. Proton transfer pathways in bacteriorhodopsin at 2.3 Å resolution. *Science.* 280:1934–1937.

Metz, G., F. Siebert, and M. Engelhard. 1992. Asp 85 is the only internal aspartic acid that gets protonated in the M intermediate and the purple-to-blue transition of bacteriorhodopsin. *FEBS Lett.* 303:237–241.

Moltke, S., and M. P. Heyn. 1995. Photovoltage kinetics of the acid-blue and acid-purple forms of bacteriorhodopsin: evidence for no net charge transfer. *Biophys. J.* 69:2066–2073.

Mowery, P. C., R. H. Lozier, Q. Chae, Y. Tseng, M. Taylor, and W. Stoeckenius. 1979. Effect of acid pH on the absorption spectra and photoreactions of bacteriorhodopsin. *Biochemistry.* 18:4100–4107.

Nasuda-Kouyama, A., K. Fukuda, T. Iio, and T. Kouyama. 1990. Effect of a light-induced pH gradient on purple-to-blue and purple-to-red transitions of bacteriorhodopsin. *Biochemistry.* 29:6778–6788.

Oesterhelt, D., and W. Stoeckenius. 1971. Rhodopsin-like protein from the purple membrane of *Halobacterium halobium*. *Nat. New Biol.* 233: 149–152.

Oesterhelt, D., and W. Stoeckenius. 1974. Isolation of the cell membrane of *Halobacterium halobium* and its fractionation into red and purple membrane. *Methods Enzymol.* 31:667–678.

Ottolenghi, M., and M. Sheves (editors). 1995. Photophysics and Photochemistry of Retinal Proteins. *Isr. J. Chem.* 35:193–515.

Padros, E., M. Duñach, and M. Sabes. 1984. Induction of the blue form of bacteriorhodopsin by low concentrations of sodium dodecyl sulfate. *Biochim. Biophys. Acta.* 769:1–7.

Pardo, E., F. Sepulcre, J. Cladera, M. Duñach, A. Labarta, J. Tejada, and E. Padros. 1998. Experimental and theoretical characterization of the high-affinity cation binding site of the purple membrane. *Biophys. J.* 75:777–784.

Pebay-Peyroula, E., G. Rummel, J. P. Rosenbusch, and E. M. Landau. 1997. X-ray structure of bacteriorhodopsin at 2.5 Å from microcrystals grown in lipidic cubic phases. *Science.* 277:1676–1681.

Stuart, J. A., B. W. Vought, C. F. Zhang, and R. R. Birge. 1995. The active site of bacteriorhodopsin. Two-photon spectroscopic evidence for a positively charged chromophore binding site mediated by calcium. *Biospectroscopy.* 1:9–28.

Szundi, I., and W. Stoeckenius. 1987. Effect of lipid surface charges on the purple-to-blue transition of bacteriorhodopsin. *Proc. Natl. Acad. Sci. U.S.A.* 84:3681–3684.

Szundi, I., and W. Stoeckenius. 1988. Purple-to-blue transition of bacteriorhodopsin in a neutral lipid environment. *Biophys. J.* 54:227–232.

Szundi, I., and W. Stoeckenius. 1989. Surface pH controls purple-to-blue transition of bacteriorhodopsin. *Biophys. J.* 56:369–383.

Tan, E. H. L., D. S. K. Govender, and R. R. Birge. 1996. Large organic cations can replace Mg^{2+} and Ca^{2+} ions in bacteriorhodopsin and maintain proton pumping ability. *J. Am. Chem. Soc.* 118:2752–2753.

Tuzi, S., S. Yamaguchi, M. Tanio, H. Konishi, S. Inoue, A. Naito, R. Needleman, J. K. Lanyi, and H. Saitô. 1999. Location of a cation binding site in the loop between helices F and G of bacteriorhodopsin, as studied by ^{13}C-NMR. *Biophys. J.* 76:1523–1531.

Váró, G., L. Brown, R. Needleman, and J. K. Lanyi. 1999. Binding of calcium ions to bacteriorhodopsin. *Biophys. J.* 76:3219–3226.

Váró, G., and J. K. Lanyi. 1989. Photoreactions of bacteriorhodopsin at acid pH. *Biophys. J.* 56:1143–1151.

Voss, J., L. Salwinski, R. Kaback, and W. L. Hubbell. 1995. A method for distance determination in proteins using a designed metal ion binding site and site-directed spin labeling: evaluation with T4 lysozyme. *Proc. Natl. Acad. Sci. U.S.A.* 92:12295–12299.

Yang, D., and M. A. El-Sayed. 1995. The Ca^{2+} binding to deionized monomerized and to retinal removed bacteriorhodopsin. *Biophys. J.* 69:2056–2059.

Yoo, S. K., E. S. Awad, and M. A. El-Sayed. 1995. Comparison between the binding of Ca^{2+} and Mg^{2+} to the two high-affinity sites of bacteriorhodopsin. *J. Phys. Chem.* 99:11600–11604.

Zhang, N. Y., and M. A. El-Sayed. 1993. The C-terminus and the Ca^{2+} low-affinity binding sites in bacteriorhodopsin. *Biochemistry*. 32: 14173–14175.

Zhang, Y. N., M. A. El-Sayed, M. L. Bonet, J. K. Lanyi, M. Chang, B. Ni, and R. Needleman. 1993. Effects of genetic replacements of charged and H-bonding residues in the retinal pocket on Ca^{2+} binding to deionized bacteriorhodopsin. *Proc. Natl. Acad. Sci. U.S.A.* 90:1445–1449.

Zhang, Y. N., L. L. Sweetman, E. S. Awad, and M. A. El-Sayed. 1992. Nature of the individual Ca^{2+} binding sites in Ca^{2+}-regenerated bacteriorhodopsin. *Biophys. J.* 61:1201–1206.